Exploiting few mode-fibers for optical time-stretch confocal microscopy in the short near-infrared window

Yi Qiu, Jingjiang Xu, Kenneth K. Y. Wong, and Kevin K. Tsia*

Department of Electrical and Electronic Engineering, The University of Hong Kong, Pokfulam Road, Hong Kong
*tsia@hku.hk

Abstract: Dispersive fiber is well-regarded as the most viable candidate for realizing efficient optical time-stretch process – an ultrafast spectroscopic measurement technique based on the wavelength-to-time mapping via group velocity dispersion (GVD). Despite optical time-stretch has been anticipated to benefit a wide range of high-throughput biomedical diagnoses, the lack of commercially-available dispersive fibers which can operate in the "biomedically-favorable" short near-infrared (~800 nm – 1100 nm) range hinders practical time-stretch-based biomedical spectroscopy and microscopy. We here explore and demonstrate the feasibility of using the standard telecommunication single-mode fibers (e.g. SMF28 and dispersion compensation fiber (DCF)) as few-mode fibers (FMFs) for optical time-stretch confocal microscopy in the 1μm range. By evaluating GVD of different FMF modes and thus the corresponding time-stretch performances, we show that the fundamental modes (LP_{01}) of SMF28 and DCF, having sufficiently high dispersion-to-loss ratios, are particularly useful for practical time-stretch spectroscopy and microscopy at 1 μm, without the need for the specialty 1 μm SMF. More intriguingly, we also show that the higher-order FMF modes (e.g. LP_{11}) could be excited and utilized for time-stretch imaging. Such additional degree of freedom creates a new avenue for optimizing and designing the time-stretch operations, such as by tailored engineering of the modal-dispersion as well as the GVD of the individual FMF modes.

©2012 Optical Society of America

OCIS codes: (170.0110) Imaging systems; (060.2350) Fiber optics imaging; (180.0180) Microscopy; (170.0180) Microscopy; (170.7160) Ultrafast technology.

References and links

1. D. R. Solli, J. Chou, and B. Jalali, "Amplified wavelength-time transformation for real-time spectroscopy," Nat. Photonics **2**(1), 48–51 (2008).
2. K. Goda, D. R. Solli, K. Tsia, and B. Jalali, "Theory of amplified dispersive Fourier transformation," Phys. Rev. A **80**(4), 043821 (2009).
3. J. Chou, D. R. Solli, and B. Jalali, "Real-time spectroscopy with subgigahertz resolution using amplified dispersive Fourier transformation," Appl. Phys. Lett. **92**(11), 111102 (2008).
4. S. Moon and D. Y. Kim, "Ultra-high-speed optical coherence tomography with a stretched pulse supercontinuum source," Opt. Express **14**(24), 11575–11584 (2006).
5. T.-J. Ahn, Y. Park, and J. Azaña, "Ultrarapid optical frequency-domain reflectometry based upon dispersion-induced time stretching: principle and applications," IEEE J. Sel. Top. Quantum Electron. **18**(1), 148–165 (2012).
6. K. Goda, K. K. Tsia, and B. Jalali, "Amplified dispersive Fourier-transform imaging for ultrafast displacement sensing and barcode reading," Appl. Phys. Lett. **93**(13), 131109 (2008).
7. A. M. Fard, A. Mahjoubfar, K. Goda, D. R. Gossett, D. Di Carlo, and B. Jalali, "Nomarski serial time-encoded amplified microscopy for high-speed contrast-enhanced imaging of transparent media," Biomed. Opt. Express **2**(12), 3387–3392 (2011).
8. K. K. Tsia, K. Goda, D. Capewell, and B. Jalali, "Performance of serial time-encoded amplified microscope," Opt. Express **18**(10), 10016–10028 (2010).

9. K. Goda, K. K. Tsia, and B. Jalali, "Serial time-encoded amplified imaging for real-time observation of fast dynamic phenomena," Nature **458**(7242), 1145–1149 (2009).
10. C. Zhang, Y. Qiu, R. Zhu, K. K. Y. Wong, and K. K. Tsia, "Serial time-encoded amplified microscopy based on picosecond supercontinuum source," Opt. Express **19**, 15810–15816 (2011).
11. T.-J. Ahn, Y. Jung, K. Oh, and D. Y. Kim, "Optical frequency-domain chromatic dispersion measurement method for higher-order modes in an optical fiber," Opt. Express **13**(25), 10040–10048 (2005).
12. F. Yaman, N. Bai, B. Zhu, T. Wang, and G. Li, "Long distance transmission in few-mode fibers," Opt. Express **18**(12), 13250–13257 (2010).
13. F. Yaman, N. Bai, Y. K. Huang, M. F. Huang, B. Zhu, T. Wang, and G. Li, "10 x 112Gb/s PDM-QPSK transmission over 5032 km in few-mode fibers," Opt. Express **18**(20), 21342–21349 (2010).
14. S. Ramachandran, "Dispersion-tailored few-mode Fibers: A versatile platform for in-fiber photonic devices," J. Lightwave Technol. **23**(11), 3426–3443 (2005).
15. T. T. W. Wong, A. K. S. Lau, K. K. Y. Wong, and K. K. Tsia, "Optical time-stretch confocal microscopy at 1um," Opt. Lett. **37**(16), 3330–3332 (2012).
16. K. Goda, A. Mahjoubfar, C. Wang, A. Fard, J. Adam, D. R. Gossett, A. Ayazi, E. Sollier, O. Malik, E. Chen, Y. Liu, R. Brown, N. Sarkhosh, D. Di Carlo, and B. Jalali, "Hybrid dispersion laser Scanner," Sci Rep **2**(445), 1–8 (2012).
17. P. Hamel, Y. Jaouën, R. Gabet, and S. Ramachandran, "Optical low-coherence reflectometry for complete chromatic dispersion characterization of few-mode fibers," Opt. Lett. **32**(9), 1029–1031 (2007).
18. S. Ramachandran, *Fiber Based Dispersion Compensation*, 1st ed. (Springer, 2007).
19. A. F. Zuluaga, R. Drezek, T. Collier, R. Lotan, M. Follen, and R. Richards-Kortum, "Contrast agents for confocal microscopy: how simple chemicals affect confocal images of normal and cancer cells in suspension," J. Biomed. Opt. **7**(3), 398–403 (2002).
20. D. Yelin, C. Boudoux, B. E. Bouma, and G. J. Tearney, "Large area confocal microscopy," Opt. Lett. **32**(9), 1102–1104 (2007).
21. K. K. Tsia, K. Goda, D. Capewell, and B. Jalali, "Simultaneous mechanical-scan-free confocal microscopy and laser microsurgery," Opt. Lett. **34**(14), 2099–2101 (2009).
22. C. Boudoux, S. Yun, W. Oh, W. White, N. Iftimia, M. Shishkov, B. Bouma, and G. Tearney, "Rapid wavelength-swept spectrally encoded confocal microscopy," Opt. Express **13**(20), 8214–8221 (2005).

1. Introduction

Optical spectral measurements and analyses are nowadays pervasive in basic life science research and clinical diagnostics, such as optical spectroscopy (e.g. absorption, fluorescence and Raman), optical coherence tomography (OCT), and hyper-spectral imaging. In spite of these technological advancements, boosting the spectral measurement speed, and thus the throughput, without compromising the accuracy has long been hindered by the fundamental tradeoff between sensitivity and speed in the traditional spectrometers. Based on an entirely different measurement strategy, dispersive Fourier transform (DFT), also known as optical time-stretch, has been developed to deliver ultrafast real-time spectral measurement with a high spectral acquisition rate as high as >MHz – a speed not achievable with conventional spectrometers [1–3]. The same technique has also found applications in high-speed optical imaging, such as OCT [4,5] and serial time-encoded amplified microscopy (STEAM), or generically called *time-stretch microscopy* [6–10]. In the time-stretch process, an optical broadband pulse is stretched in time by group velocity dispersion (GVD) in a way that its spectral information is mapped into time. It thus facilitates ultrafast real-time spectral measurements by using a high-speed electronic digitizer, instead of the conventional spectrometer.

The common time-stretch operation wavelength range has been focused on the telecommunication wavelength band (~1550 nm) because of the wide availability of low-loss and dispersive single-mode fibers (SMFs) for this band – the central element for the time-stretch process [1–10]. Extending the utility of the time-stretch process to the spectral window favorable for biomedical diagnostics, i.e. the shorter near-infrared (NIR) range (loosely defined as ~800 – ~1100 nm), has in contrast been regarded to be challenging because of the lack of the low-cost and dispersive 1 μm SMFs. In this paper, we demonstrate that the standard telecommunication fibers (e.g. SMF28 and dispersion compensation fiber (DCF)) can be exploited as the few-mode fibers (FMFs) in this NIR range for realizing cost-effective and efficient time-stretch confocal microscopy in the 1 μm window. Multi-mode fibers should

generally be avoided in the time-stretch process because the coexistence of modal dispersion and GVD leads to the ambiguity in the wavelength-time mapping. Nevertheless, the fact that the FMF does not support excessive number of fiber modes renders selective mode excitation efficient under the proper input coupling conditions [11–14]. Indeed, FMF has been proven to be effective for low-loss and long-distance data transmission in fiber-optic communication with negligible modal coupling [12, 13] – a feature particularly encouraging for achieving high-dispersion, and thus high-resolution time stretch microscopy. We here show that the fundamental (LP_{01}) FMF modes can be excited and exhibit sufficiently large GVD for time-stretch microscopy with cellular resolution. We also report that it is possible to utilize the higher-order (LP_{11}) mode for time-stretch microscopy, albeit the presence of the image ghosting effect. In order to evaluate the imaging performance, we experimentally characterized the dispersive properties of the fiber modes in the 1-μm SMF and two types of FMFs, which are SMF28 and DCF. We show that the LP_{01} modes of the SMF28 and the DCF, having high dispersion-to-loss ratios, are the viable candidates for practical time-stretch spectroscopy and microscopy at 1 μm. Without resorting to the specialty dispersive SMFs in this NIR range [15], the use of FMFs could also open up additional degrees of freedom for designing and optimizing the optical time-stretch system, e.g. by using a wide variety of modal-dispersion engineered FMFs [14]. For instance, tailoring the high-order modes in a FMF with desired dispersive properties (e.g. group delays, dispersions, and dispersion slopes) can be implemented achieved by fabricating the FMF with a core refractive-index profile which is favorable for guiding a particular high-order mode. Further control of mode selection can be attained by integrating the FMF with the long-period fiber gratings (LPGs), which can be designed to serve as broadband mode converters [14].
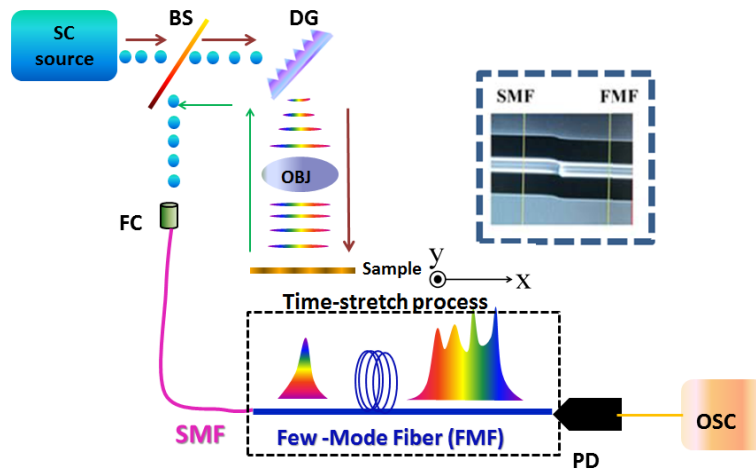
2. Experimental set-up

Fig. 1. (a) Experimental set up of time-stretch confocal microscopy at 1μm using FMF. Right upper inset: an image of the fused fiber (between a SMF and a FMF). The controlled offset between the two fibers can be observed at the connecting facets. SC: supercontimuum, BS: beam splitter, DG: transmission diffraction grating, OBJ: objective lens, FC: fiber collimator, PD: photodetector, OSC: real-time oscilloscope.

In time-stretch confocal microscopy, the spatial coordinates of the specimen are first encoded in the wavelength spectrum of a broadband pulse with a "spectral shower" created by a spatial disperser, e.g. diffraction grating (DG) [6–10]. The pulse is then time-stretched by GVD in a dispersive fiber (i.e. FMFs in our case) so that the image-encoded spectrum is mapped into the serial temporal waveform which is finally captured by the electronic digitizer in real time. In our setup (Fig. 1), the broadband source is a supercontinuum (SC) (~900nm – 1300nm)

generated by a 20-m long photonic crystal fiber (PCF), which is pumped by a mode-locked laser (center wavelength = 1064nm and pulse width = 9ps). A transmission DG with a groove density of 1200 lines/mm and an objective lens (NA = 0.66) are employed to focus the one-dimensional (1D) spectral shower onto the sample [6–10, 15]. The back-scattered spectral shower is collected by a short SMF (~1 m) which is fused with the FMF. Finally, the time-stretched signal generated in the FMF is captured by a real-time oscilloscope (16 GHz, 80 GS/s). Note that the aperture of the SMF serves as the pinhole providing the confocal imaging feature. The entire 2D images can be obtained by line-scanning of the sample or the spectral shower in the orthogonal direction (*y*-direction in Fig. 1). We emphasize that this 1D line-scan mode can readily be applied in high-speed flow cell imaging (at a MHz line-scan rate), in which the unidirectional cell flow automatically facilitates all the 1D line-scans of individual cells without beam scanning of the spectral shower [7, 9, 16].

Selective modal excitation in the FMF is done by introducing different lateral offsets between the fiber facets of the input 1μm SMF and the FMF using the standard fusion splicer. In general, fundamental mode LP_{01} in the two FMFs (SMF28 and DCF) can be easily excited when there is no offset between the two fibers. In contrast, the higher-order LP_{11} mode in the SMF28 can be observed when an offset is introduced (Inset in Fig. 1).

3. Experimental results

3.1 Characterizations of the GVD and the wavelength-time mapping

The same time-stretch technique can also be utilized for characterizing the GVD of different FMF modes. This is simply based on the relation $\delta\tau = D(\lambda_o)\cdot L\cdot\Delta\lambda$, where $\Delta\lambda$ is the bandwidth of the input source to the FMF (in nm), L is the length of the FMF (in km), $D(\lambda_o)$ is the GVD at the center wavelength λ_o (in ps/nm-km) and $\delta\tau$ is the temporal duration of the time-stretched pulse. Having excited the particular FMF mode, we can readily measure the corresponding $\delta\tau$ and thus obtain $D(\lambda_o)$ for an input bandwidth $\Delta\lambda$ centered at λ_o. The complete GVD profile as a function of wavelength can then be obtained by scanning the bandpassed spectrum across the SC (1050 nm – 1140 nm) using a tunable filter, which is based on a grating-pair configuration with a filtered bandwidth of 8 nm in our case (see Fig. 2(a)). Compared to the previously reported methods [11,17], this time-stretch approach, without the need for interferometric configurations, provides a simple and straightforward *in-line* measurement of the GVD of the individual FMF modes using the same time-stretch microscopy setup. We verified the fiber modes by imaging the fiber output mode patterns using the NIR camera (Figs. 2(b)-2(e)). The alignment was also checked by monitoring the interference fringe pattern in the spectrum – a consequence of the beating between the LP_{01} mode and the higher-order LP_{11} mode [11–13,17]. The fringes vanish when the two fibers are well-aligned, indicating that only the fundamental mode (LP_{01}) of the FMF is excited (see the blue curve in Fig. 2(f)).
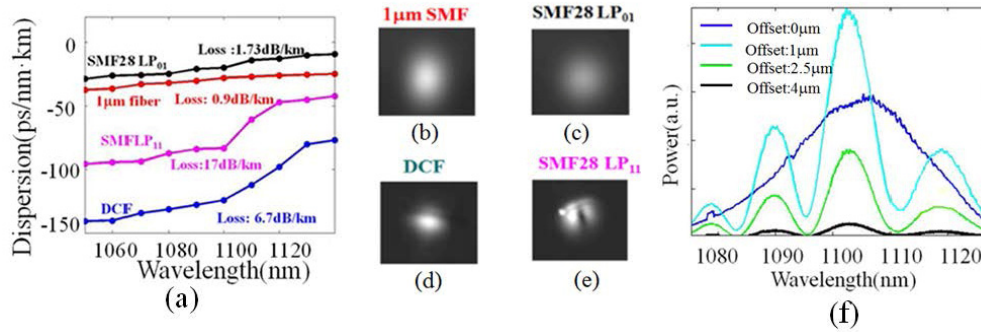
Fig. 2. (a) Measured GVD curves and the loss values of different fiber modes in the FMFs and the 1μm SMF. (b)-(e) Captured images of the fiber output mode patterns using the NIR camera. (f) Measured output spectra of the SMF28 when an alignment offset is varied at the fiber input. The fringes are attributed to the beating between the fundamental mode (LP_{01}) and higher-order mode (LP_{11}).

The spatial resolution in time-stretch microscopy can be governed by three limiting regimes, each of which is dominated by (i) the spectral resolution of the DG (spatial-dispersion limited), (ii) the spectral resolution defined by stationary-phase approximation (SPA) in the time-stretch process (SPA-limited), or (iii) the temporal resolution of the digitizer (digitizer-limited) [8]. The highest resolution, i.e. spatial-dispersion-limited resolution, is only achievable when GVD is sufficiently large [8]. However, large GVD intrinsically comes along with dispersive loss which degrades the signal-to-noise ratio, and thus the detection sensitivity. In this regard, a metric which can indicate the trade-off between the GVD and loss should be used to evaluate the *effectiveness* of the time-stretch process, i.e. GVD-to-loss ratio R (in ps/nm-dB). From Fig. 2(a), the LP_{01} mode of the SMF28 has the R-ratios of ~10 ps/nm-dB, about one-third of that of the 1μm-SMF, i.e. ~33 ps/nm-dB. By selectively exciting the higher-order LP_{11} mode in SMF28, we can achieve much higher GVD (~75 ps/nm·km), it however comes at the expense of a significant fiber loss (~17dB/km), resulting in an R-ratio of only 4 ps/nm-dB. Surprisingly, we observed that the R-ratio of the LP_{01} mode in the DCF is as high as ~18 ps/nm-dB – showing a reasonably large dispersion with low loss at 1μm for practical FMF-based time-stretch microscopy. The comparison of the R-ratio and other related parameters among different cases are summarized in Table 1.

Table 1. Key specifications of different fiber modes investigated in the experiment, namely the GVD, fiber loss, the fiber length, total dispersion and the GVD-to-loss ratio R. Note that the GVD and the total dispersion are the average values taken across the spectrum of 1050 nm – 1140 nm.

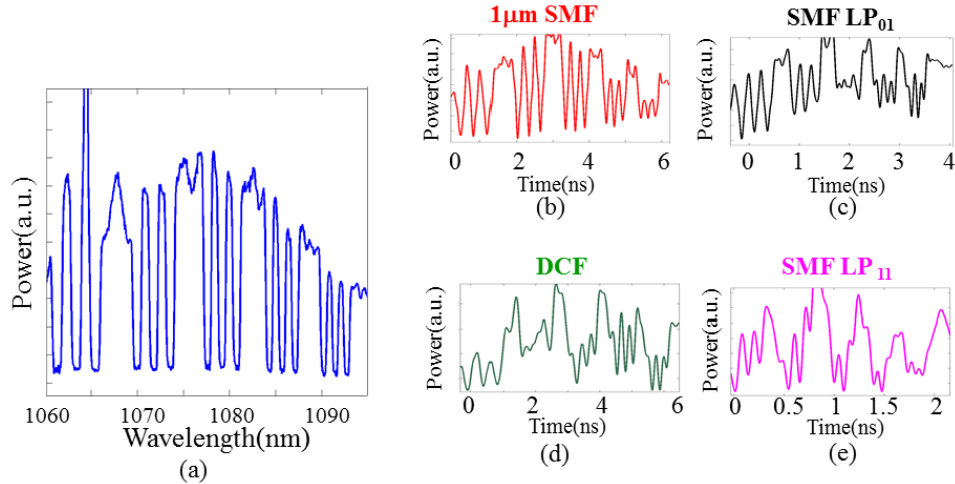|	Fiber mode	GVD (ps/nm-km)	Loss (dB/km)	Length (km)	Total dispersion (ps/nm)	GVD-to-loss ratio R (ps/nm-dB)
1μm SMF	LP_{01}	30	0.9	5	150	33
SMF28	LP_{01}	17	1.7	6	102	10
SMF28	LP_{11}	75	17.0	0.35	26	4
DCF	LP_{01}	120	6.7	1.44	178	18

Fig. 3. Wavelength-to-time mapping based on different FMF modes as well as the 1μm SMF. (a) The input shaped spectrum to the fiber-under-test. The time-stretched signals of (b) 1μm SMF, (c) LP_{01} of SMF28, (d) LP_{01} of DCF and (e) LP_{11} of SMF28. The input misalignment offset is 4 mm in (d). Note that all the spectral information can in general be mapped into time well within few ns in all of the cases – demonstrating the ultrafast spectral acquisition speed enabled by the time-stretch process.

Having characterized the GVD values of different fiber modes, we then evaluated their time-stretch performances by comparing the corresponding wavelength-to-time mappings (Figs. 3(b)-3(e)) given a shaped input SC spectrum, which was generated by a grating-pair spectral shaper (Fig. 3(a)). The length of each fiber was chosen to achieve a reasonable balance between the total dispersion and loss (Table 1). From Fig. 3, the LP_{01} modes of the three fibers (i.e. 1μm SMF, SMF28 and DCF), which all have the comparable total dispersion as high as ~100 – 160 ps/nm, generally show the unambiguous one-to-one wavelength-to-time mapping and are able to resolve most of the spectral features. In contrast, the mapping of the LP_{11} mode of SMF28, with a much smaller dispersion of ~26 ps/nm, is relatively unclear. Such comparison can further be explained as follow. The spectral resolution achieved in the time-stretch process is defined as $\delta\lambda = \max\left\{\delta\lambda_{SPA}, \delta\lambda_{dig}\right\}$, where $\delta\lambda_{SPA} = \lambda\sqrt{2/D \cdot L \cdot c}$ is the spectral resolution defined by the SPA in the time-stretch process and $\delta\lambda_{dig} = 0.35/\left(D \cdot L \cdot f_{dig}\right)$ is the spectral resolution determined by the detection bandwidth of the system (i.e. the photodetector and the digitizer) [2,8]. D is the GVD (in ps/nm-km), f_{dig} is the total detection bandwidth of the system (~10 GHz in our case), and c is the speed of light. Based on the specifications shown in Table 1, we can calculate the spectral resolution of the LP_{01} modes in the 1μm-SMF, SMF28 and DCF, which is ~0.26 – 0.4 nm. This is much smaller than that of the LP_{11} mode in SMF28, i.e. ~1.6 nm. This is consistent with that the time-stretched waveform of the LP_{11} mode can barely resolve the spectral lines in the shaped SC spectrum, which has the minimum line width of ~1 nm (Fig. 3(e)). The unclear mapping can also be attributed to the modal coupling in the fiber, which is evident from the beating effect shown in Fig. 2(f). As a result, not only GVD contributes to the time-stretch process, but so does the modal dispersion as well. Consequently, the wavelength-to-time mapping is no longer one-to-one and the original spectral information thus becomes obscured in the time domain. We note that the intrinsic dispersive loss can be circumvented by optically amplifying the time-stretched signal either using distributed Raman amplification in the same fiber [1–3,6–10] or the discrete optical amplifiers, which are commonly available in the 1 μm range (e.g.(Ytterbium doped fiber amplifier) YDFA, and semiconductor optical amplifiers).

3.2 FMF-based time-stretch confocal microscopy

We performed time-stretch confocal microscopy to image a resolution target (USAF-1951) based on different fiber modes in the FMFs and the 1μm SMF (Figs. 4(a)-4(d)). By performing 200 line-scans with a step size of 0.5 μm (along the *y*-direction), the field-of-view (FOV) is as large as ~0.44 mm × 0.1 mm. The captured time-stretch images based on the LP_{01} modes in the SMF28 and DCF (Figs. 4(b)-4(c)) show the similar image quality compared with that using 1μm SMF (Fig. 4(a)) and resolve well the smallest line feature (a linewidth of 2μm in Group 7). As mentioned before, the spatial resolution of time-stretch
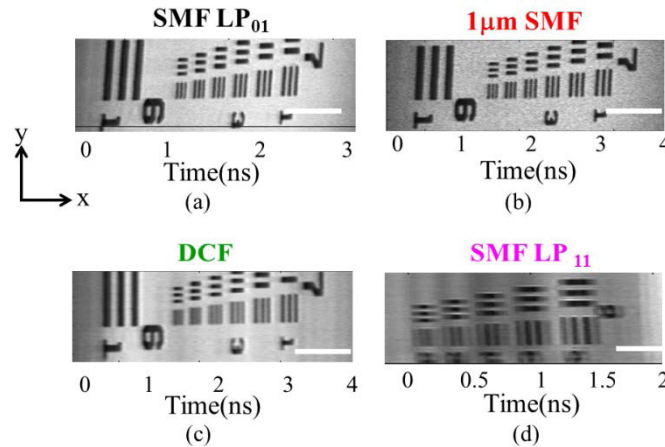

Fig. 4. Time-stretch confocal images of a resolution target (USAF-1951) captured based on different fiber modes: (a) LP_{01} mode of a 9km-long SMF28, (b) LP_{01} mode of a 5 km-long 1μm SMF, (c) LP_{01} mode of a 1.44km-long DCF, and (d) LP_{11} mode of a 0.35km-long SMF 28. The input misalignment offset is 4 μm in (d). The scale bars represent 50 μm in (a)-(c), and 100μm in (d)

microscopy is determined by the three limiting cases: (1) spatial-dispersion limited δx_{sd}, (ii) SPA-limited δx_{SPA}, or (iii) digitizer-limited δx_{dig}. The actual resolution δx is thus the maximum value in the three cases, i.e. $\delta x = \max\{\delta x_{sd}, \delta x_{SPA}, \delta x_{dig}\}$. Table 2 summarizes the resolution values of each limiting case based on different fiber modes. Time-stretch imaging based on the LP_{01} modes in SMF28 and DCF achieves the resolution of ~2μm, which is primarily digitizer-limited. As we show later that this resolution is high enough for cellular imaging based on time-stretch microscopy. The highest resolution, i.e. the spatial-dispersion-limited resolution, can be attained if the dispersion is further enhanced > 180 ps/nm. This can be achieved by using a longer fiber in conjunction with the optical amplification to compensate the inherent dispersive loss. Indeed, an incredibly large dispersion of > 10ns/nm has been demonstrated in time-stretch spectroscopy [3]. It should be emphasized that all the time-stretch images were captured here at an ultrafast spectral acquisition rate (i.e. line-scan rate) of 10 MHz, determined by the repetition rate of the SC source. This is orders-of-magnitude faster than that achievable in the conventional spectrometers. In addition, each single-shot line scan (along the *x*-direction) of the time-stretch image is obtained only within few ns (i.e. a duty cycle of ~4% given a scan rate of 10MHz), determined by the GVD and the illumination bandwidth. Such duty cycle is already sufficient for achieve high-resolution time-stretch imaging.

Table 2. Three different limiting regimes governing the spatial resolution of time-stretch microscopy based on different fiber modes. The final resolution is defined as $\delta x = \max\{ \delta x_{sd},\ \delta x_{SPA},\ \delta x_{dig}\}$, where $\delta x_{SPA} = C \cdot \delta\lambda_{SPA}$ and $\delta x_{dig} = C \cdot \delta\lambda_{dig}$. C is the conversion factor between the space and wavelength [9].

	Fiber mode	Spatial-dispersion-limited resolution δx_{sd} (µm)	SPA-limited resolution $\delta x_{SPA} = C \cdot \delta\lambda_{SPA}$ (µm)	Digitzer-limited resolution $\delta x_{dig} = C \cdot \delta\lambda_{dig}$ (µm)
1µm SMF	LP_{01}	1.5	1.6	1.8
SMF28	LP_{01}	1.5	1.9	2.4
SMF28	LP_{11}	1.5	3	6
DCF	LP_{01}	1.5	1.5	1.6

Interestingly, despite of having the limited dispersion, time-stretch imaging based on the LP_{11} mode in SMF28 (Fig. 4(d)) is also possible with a limited resolving power, i.e. being able to resolve a minimum linewidth of 15µm (Group 6 of the resolution target). In addition, image quality is also affected by the "ghosting effect". Such ghosting effect indicates that the presence of ambiguous wavelength-time mapping during the time-stretch process, i.e. one wavelength can be mapped to more than one time points. We here attribute two possible mechanisms resulting in such mapping ambiguity: (1) mode coupling and (2) polarization mode dispersion (PMD) of the degenerate LP11 modes due to perturbation along the FMF [18]. Despite of the ghosting effect, the image in Fig. 4(d) should be predominantly contributed by LP11 mode. It can be evident from the measured loss of this image, which considerably higher than other images based on LP01 modes (Figs. 4(a)-4(c)). Moreover, the GVD estimated from the FOV of the image in Fig. 4(d) is in excellent agreement with the GVD of the LP11 mode measured in Fig. 2(a).

The above results thus clearly show the feasibility of selectively exciting and utilizing the LP_{01} mode in the FMF for efficient time-stretch confocal microscopy. Moreover, the fact that the higher-order FMF modes can also be employed for time-stretch imaging offers an additional degree of freedom for realizing time-stretch imaging. Albeit the complication introduced by the modal coupling, we anticipate that careful modal dispersion and GVD engineering of FMFs [14] can open up a wide variety of opportunities for optimizing the time-stretch imaging performance based on either the LP_{01} mode or the higher-order modes in FMFs.
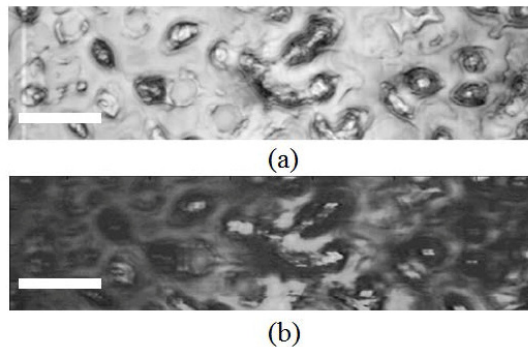

(a)

(b)

Fig. 5. Raw images of the nasopharyngeal epithelial cells captured by (a) the spectrally-encoding approach, and (b) time-stretch confocal microscopy based on the LP_{01} mode of a 6km SMF28. The scale bars represent 50 µm.

We also demonstrated cellular imaging using FMF-based time-stretch microscopy (based on the LP_{01} mode in a 6-km SMF28). The specimen is the nasopharyngeal epithelial cell lines, which were treated with methanol and 6% acetic acid before fixation to increase the image contrast of the nuclei [19]. Clearly, the time-stretch image is able to reveal the cellular structures, such as the nuclei (Fig. 5(b)). For comparison, we also performed the imaging of the same specimen based on spectral-encoding [20–22], i.e. the spectrally-encoded information is directed to the spectrometer without undergoing the time-stretch process in the FMFs (Fig. 5(a)). We emphasize that the spectrally-encoded image was captured by a spectrometer at a spectral acquisition rate of 5 Hz whereas the time-stretch image, with a comparable image quality, is captured at an order-of-magnitude higher speed – a core feature of time-stretch confocal microscopy.

4. Conclusion

In summary, we demonstrated time-stretch confocal microscopy in the 1-μm spectral range, a favorable window for biomedical diagnostics, by using the standard telecommunication SMFs (SMF28 and DCF) as the FMFs instead of the high-cost specialty 1-μm SMF. The fact that FMF can support a small number of modes (typically 2-3 modes) renders it as a versatile platform of exploiting any particular fiber mode for the time-stretch process by selective modal excitation. Specifically, we showed that the LP_{01} modes in the SMF28 and DCF exhibit sufficiently high dispersion, and can thus be utilized for high-resolution time-stretch imaging. In addition, we showed that the higher-order FMF mode can also be exploited for time-stretch microscopy, albeit the complication possibly introduced by the mode coupling and PMD. This result opens up a wide variety of opportunities of further optimizing the time-stretch process by e.g. modal dispersion engineering as well as the GVD engineering of the FMFs [14]. It should also be emphasized that the intrinsic dispersive fiber in all the above cases can be readily circumvented by distributed fiber Raman amplification during the time-stretch process [1–3,6–10], or using the discrete optical amplifiers, which are commonly available in the 1 μm range (e.g. YDFA, and semiconductor optical amplifiers), to optically amplify the image signal. It is of great importance in realizing high-speed and high-sensitivity time-stretch-based spectroscopy and microscopy for the high-throughput diagnostic applications, e.g. imaging flow-cytometry.